Cite this article as:
S. Lima, R. E.I. García-López, A. Adawy, G. Marcì, F. Scargiali, Valorisation of *Chlorella sp.* biomass in 5-HMF through a two-step conversion in the presence of Nb_2O_5 and $NbOPO_4$ and optimisation through *reactive* extraction, *Chemical Engineering Journal*, Available online 3 July 2023
https://doi.org/10.1016/j.cej.2023.144583

Valorisation of *Chlorella sp.* biomass in 5-HMF through a two-step conversion in the presence of Nb_2O_5 and $NbOPO_4$ and optimisation through *reactive* extraction

Serena Lima[a], Elisa I. García-López[b]*, Alaa Adawy[c], Giuseppe Marcì[a] , Francesca Scargiali [a]

[a]Università di Palermo, Dipartimento di Ingegneria, Viale delle Scienze Ed. 6, 90128 Palermo, Italy

[b]Università di Palermo, STEBICEF, Viale delle Scienze Ed. 16, 90128 Palermo, Italy

[c]Unit of Electron Microscopy and Nanotechnology, Institute for Scientific and Technological Resources (SCTs), University of Oviedo, 33006, Oviedo, Spain

*corresponding author: elisaisabel.garcialopez@unipa.it

Abstract

The valorisation of recalcitrant *Chlorella sp.* microalgal biomass by the extraction of the sugar content and its conversion into 5-hydroxymethyl furfural (5-HMF) has been carried out in two-steps. In the first step, a pre-treatment of the biomass was optimized to obtain, by sonication and hydrothermal treatments also in the presence of acetic acid and SiO_2 pellets, the maximum release of carbohydrate and their hydrolysis to monosaccharides. The second step, carried out under hydrothermal conditions, was devoted to the heterogeneous catalytic isomerisation/dehydration of the monosaccharides (essentially glucose and fructose) released from algae in the first reaction step to yield 5-HMF in presence of two commercial samples of niobium-based catalysts that were characterized with several techniques like specific surface area and superficial acidity measurements, SEM, FTIR and Raman. Other important features of the two catalysts are largely present in the literature due to the fact that they are commercial materials. The isomerisation/dehydration reactions of the monosaccharides proceed through a tandem pathway involving the Lewis and Brønsted acid sites provided by the surface of the acidic solids giving rise to the isomerization of glucose to fructose, followed by dehydration of fructose to 5-HMF. The optimisation of the reaction conditions was carried out in the presence of Nb_2O_5 by using a Design of Experiment (DoE) approach. The optimised parameters were identified as temperature 210 °C and 4.45 h of reaction time, providing a yield to 5-HMF of about 18% on the total sugars contained in the algae. A further optimisation has been achieved in the presence of $NbOPO_4$ instead of Nb_2O_5, which still led to 21% yield to 5-HMF on the total sugars. Moreover, using an H_2O/MIBK system, a reactive extraction was performed, obtaining the very good value of yield to 5-HMF of 29% on total sugars. In this way, a multi-approach process optimisation was performed, in line with the principles of process intensification, with the aim of improving the energy-efficiency of the entire process.

Keywords: Microalgae, Biomass valorisation, heterogeneous catalysis, Acid solid, 5-HMF, DoE

1. Introduction

Microalgae represent an interesting raw biomass compared to land plants for their ability to grow in non-arable lands, in wastewater and seawater. They are generally easy to cultivate and, especially if triggered, they may produce high-value compounds of interest for various sectors such as pharmaceutics or cosmetics [1,2]. Moreover, microalgae may well be applied in wastewater treatment, as they can employ nitrogen and phosphorous contained in wastewater efficiently [3,4]. In the last few years, the concept of microalgal biorefinery has developed. This term denotes the integration of multiple processes for the exploitation of different fractions of microalgal cells. A significant example may be the recovery of the residual cellulosic microalgal biomass fraction after the extraction of the lipids. Several reviews have been recently published concerning microalgal biorefinery [5,6]; however, the practice is still not widely applied on a pilot scale. One of the possible reasons may be that doubts have been raised about the actual decrease in costs [7]. Furthermore, the recovery of the residual cellulosic biomass usually takes place through thermochemical processes such as pyrolysis, gasification, liquefaction, or unit operations such as fermentation or anaerobic digestion, all procedures in which the economic added value is limited. [8,9].

One of the main obstacles for exploiting microalgal carbohydrates, similarly than for other lignocellulosic biomasses, is the hydrolyzation of polysaccharides to monosaccharides. This may be due to the structure of the cell, which in *Chlorella sp.* is composed of a single microfibrillar layer along with a rigid outer trilaminar layer made of algaenan, a non-hydrolyzable biopolymer. The first contains cellulose and hemicellulose, while the second extracellular protein and other carbohydrates [10,11]. Furthermore, some starch may be accumulated inside the cell. Therefore, the cell wall structure and composition deeply influence the hydrolysis of the mentioned polymers to obtain monomers. The rigidity of the cell wall can be attributed to the high levels of polysaccharides in its structure, as in *Chlorella zofingiensis*, or to the presence of a complex composition in sugars, including arabinose, galactose, rhaminose, mannose and xylose, as in *Tetraselmis suecia* and *T. striata*. Alternatively, the cell wall stiffness can be associated with the presence of algaenan or sporopollein, which can be found in some species such as *Chlorella sp* [12].

To facilitate the cleavage of the wall cell, its next disruption, and finally, the hydrolysis of the polymers it is composed of, it is often needed to pre-treat the microalgal biomass. Several pre-treatments are now available, distinguished in mechanical, physical and chemical methods. Mechanical and physical treatments may include ball milling, microwave irradiation, sonication, or thermal treatments. As an alternative, several solvents, such as acids, alkali etc. may be employed together with enzymatic methods [12,13].

Considering that the recovery of residual cellulosic algal biomass via thermochemical or fermentative processes is not convenient, a promising alternative may be the catalytic conversion of the residual sugars in furanic compounds, such as 5-hydroxy-methylfurfural (5-HMF). This molecule is produced from the dehydration of C6 sugars (glucose, fructose) and it is considered a platform chemical, being the biomass-based alternative for the synthesis of polymers, pharmaceuticals, agrochemicals, flavours and fragrances, macro- and heterocycles as well as it may be a precursor for fuel components [14]. 5-HMF is produced from the dehydration of fructose, which in turn may isomerise from glucose in the presence of acidic heterogeneous catalysts [15].

The chemical treatment of lignocellulosic biomass can yield several compounds that can be converted into different platform chemicals. In the microalgal carbohydrate residual fraction, the hemicellulose, composed of pentoses and hexoses, can be hydrolysed in C_5 and C_6 sugars and subsequently dehydrated in furfural and 5-HMF, while the cellulose, composed only of C_6 substrates, can be hydrolysed in glucose, which isomerizes in fructose and is subsequently dehydrated to 5-HMF [16]. Further steps of the process are the reactions leading to the degradation of the furanic species, such as the condensation reaction of 5-HMF which gives rise to the formation of insoluble humins and/or the 5-HMF hydration which results in the formation of levulinic acid and formic acid, as shown in Figure 1.

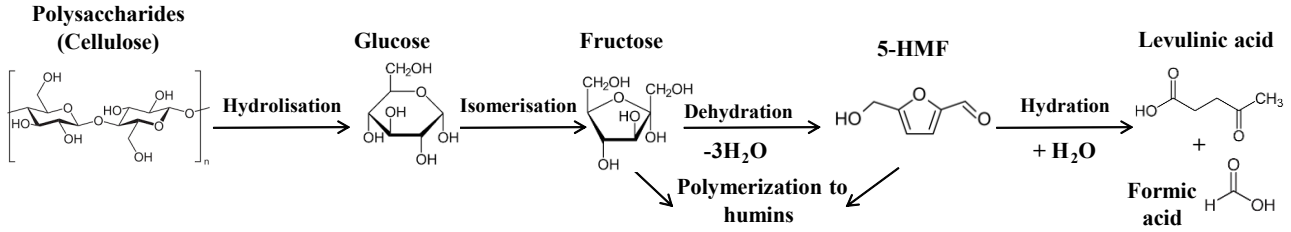

Figure 1: Scheme of the reaction for 5-HMF production from the cellulose provided by the algae.

As reported in Figure 1, 5-HMF can be obtained from glucose by stepwise isomerisation and dehydration stages. These two reactions require an acidic medium and various materials have been tested as acidic catalysts, including homogeneous and heterogeneous presenting both Lewis and Brønsted acid sites. The employment of a solid catalyst is to prefer with respect to homogeneous one, such as mineral acids as HCl or H_2SO_4, for environmental reasons, health risks and special disposal necessities. Furthermore, solid catalysts may be reused and therefore represent a more eco-sustainable alternative to mineral acids.

In the current research commercial amorphous Nb_2O_5 (niobic acid) and $NbOPO_4$ (niobium phosphate) were used as catalysts in the valorisation of the algae by the isomerisation/dehydration steps reported in Figure 1. The reaction of dehydration of fructose to 5-HMF has been successfully carried out in aqueous suspension of Nb_2O_5-based catalysts [17]. Nb_2O_5 is a well-known acidic catalyst. It is an abundant material, water-tolerant non-toxic material, with strong redox ability, Brønsted acid sites (BASs) and also Lewis acid sites (LASs) [18]. The hydrated niobium pentoxide ($Nb_2O_5 \cdot nH_2O$), known also as niobic acid, is a white polymeric amorphous material with a variable composition owing to the inconstancy of its water content which varies depending on the method of preparation and drying. It is also represented as an isopolyacid $H_8Nb_6O_{19}$, as shown in Figure 2 (A), possessing strong acidic properties and exhibiting high catalytic performances for acid-catalysed reactions. The precursor used for the oxide synthesis as well as impurities and preparation method strongly influence its physical-chemical properties [19]. By heating the hydrated isopolyacid it loses water forming stoichiometric hydrates. The amorphous solid, called also γ-niobic isopolyacid, exists up to 435 °C. Literature reports the use of Nb_2O_5 in the catalytic glucose valorisation pointing out that the LASs are responsible for the isomerization of glucose into fructose, while the BASs have an active effect on the dehydration of fructose to 5-HMF. An excess of LASs may have a deleterious effect on the 5-HMF yield due to the formation of by-products, as shown in Figure 1 [20]. In Figure 2 (A) the Brønsted (BASs) and Lewis (LASs) acid sites of niobic acid are also schematised.

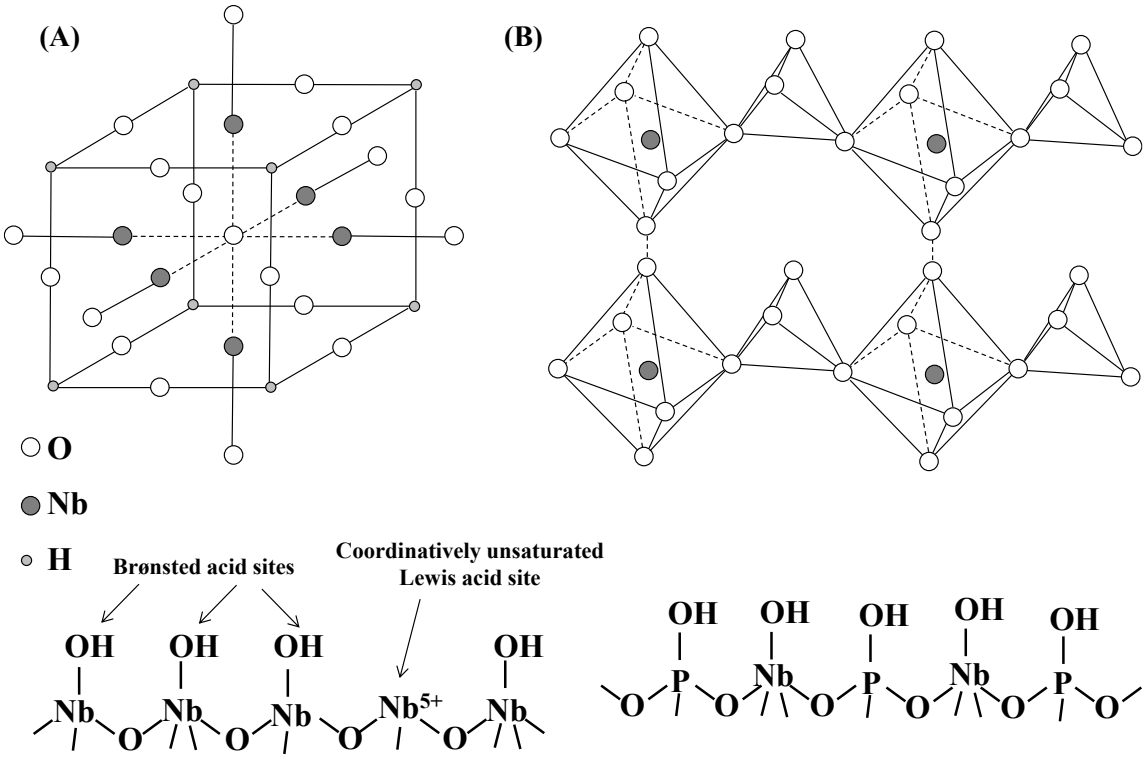

Figure 2: Structure of (A) the niobic acid cluster, $H_8Nb_6O_{19}$, representative of the Nb_2O_5 commercial catalyst HY-340 and of (B) $NbOPO_4$ polymer, where P atoms are closed on the tetrahedral structures. A representation of Brønsted and Lewis acidic sites are also shown.

Niobium oxyphosphate, $NbOPO_4$, possesses a lamellar structure constituted by layers consisting of distorted NbO_6 octahedra and regular PO_4 tetrahedra, as shown in Figure 2 (B). The four equatorial Nb-O bonds are roughly parallel to the layers making the infinite Nb-O-P linkage of the layers [21]. Each layer interacts with the others by hydrogen bonding, allowing the occlusion of neutral molecules, for example water. Consequently, this solid is behaved a water-tolerant bifunctional catalyst [22] possessing surface phosphate groups providing both Brønsted and Lewis acid sites, as shown in figure 2 (B), attributed to the penta-coordinated Nb sites [23]. Literature reports that the transformation of glucose to 5-HMF carried out in the presence of the $NbOPO_4$ catalyst leads to better catalytic yields to 5-HMF compared to the use of niobium oxide. This result is explained in terms of superior textural, catalytic and acidic properties, in addition to a higher number of BASs [24,25].
Considering that it has been stated that in the conversion of cellulose to 5-HMF the reaction of hydrolysation (see Figure 1) is the slowest stage [26], in this work the conversion of microalgal biomass into 5-HMF has been carried out in two-steps. Notably, the chosen alga was an autochthonous strain of *Chlorella sp*, previously isolated [27], which resulted recalcitrant to hydrolysation. In the first step, a pre-treatment of the biomass was optimized to obtain the maximum release of monomers. The second step was devoted to the heterogeneous catalytic isomerisation/dehydration of the C_6 monosaccharides (glucose/fructose) to obtain 5-HMF in the presence of Nb_2O_5. This second stage of the overall transformation was optimised through a Design of Experiment (DoE) approach. A further optimisation of the second step of the process has been achieved through the use of $NbOPO_4$ instead of Nb_2O_5. Moreover, the reaction was also carried out in a biphasic system in which the chemical reaction takes place in the aqueous phase, while the simultaneous separation of 5-HMF occurs in methyl isobutyl ketone used as extractive phase. In this

way, a reactive extraction was performed, in line with the principles of process intensification, with the aim of improving the energy-efficiency of the entire process. Consequently, this work reports an early-stage process for the valorisation of the polysaccharides contained in a recalcitrant microalgal biomass. The results obtained are very encouraging because, under the optimized operational conditions, a yield to 5-HMF of ca. of 29% with respect to the total sugars content present in the algal biomass was achieved.

2. Materials and Methods

2.1. Algal growth and analysis of the sugars content of the biomass

Microalga *Chlorella sp*. Pozzillo was previously isolated from Sicilian littoral and molecularly characterized [27]. The strain was kept in liquid medium. For this work, a commercial fertilizer (Spray-feed, Pavoni) diluted in H_2O was employed at the concentration of 3 g L^{-1}. A pre-culture of the microalgae was set up by inoculating 50 mL of sample from a culture flask in 500 mL of fresh medium. When cells were in late exponential phase (after about 10 cultivation days), the cell suspension were used to inoculate a bubble column photobioreactor with the volume of 5 L. The algae were cultivated for 15 days under a photon flux density of about 300 µmol m^{-2} s^{-1}. Light intensity was measured with a Delta Ohm-HD 9021 quantometer equipped with a Photosynthetic Active Radiation (PAR) probe (Delta Ohm LP 9021 PAR). After the cultivation, the biomass was harvested by centrifugation and the obtained biomass was frozen in liquid nitrogen and freeze-dried for 24 h in a bench lyophilizator (Alpha 1-2 LDplus, Christ, DE). The biomass obtained from several cultivations was collected and homogenised.

For the quantification of total monosaccharides content, an acidic hydrolysis on the whole biomass was performed by adding 24 mL of HCl 2 N and 240 mg of SiO_2 pellets (0.2-0.5 mm size) to 40 mg of biomass in a stainless-steel autoclave hydrothermal reactor (Tefic Biotech Co. Limited, Xi'an, China) with a 50 mL PTFE chamber. The autoclave was placed in a thermostatic, preheated synthetic oil bath, posed on a heated magnetic stirrer. The reactions proceeded under continuous mixing with a magnetic bar at 500 rpm; after reaction completion, the reactor was rapidly cooled using tap water. The hydrolysis was performed at 120 °C for 3 h. The suspension was filtered through 0.2 µm membranes (CA, Millipore) and sugars were analyzed by means of a HPLC Dionex UltiMate 3000 equipped with a column Rezex ROA-Organic acid H^+ operating at 60 °C and using 0.6 mL·min^{-1} of a 5 mM H_2SO_4 aqueous solution as eluent.

2.2. Biomass pre-treatments

As previously explained, in order to valorize the microalgae biomass it was necessary a preliminary treatment aimed to break down the membrane of the algae cells in order to release and hydrolyze the carbohydrates to obtain C_6 and C_5 sugars in solution. For this aim, the biomass of *Chlorella sp*. was subjected to various pre-treatments in order to find the best conditions, i.e. those which yielded the greatest quantity of sugars in solution. It is important to underline that the conditions studied here were different from those reported in section 2.1 that gave rise the highest amount of sugars. In fact, here we have tried to obtain the greatest possible release of sugars in solution avoiding the use of concentrated HCl (2 N) aqueous solution.

Different experimental settings, such as sonication, hydrothermal treatment, acidic hydrolysis with diluted acetic acid water solution were tested in combination or alone. The biomass hydrothermal treatments were performed in the same autoclave described in section 2.1. Each pre-treatment was performed on the same batch of *Chlorella sp*. by treating 40 mg of lyophilised algae dispersed in 24 mL of suspension. For each treatment two different conditions were applied by changing the

temperature and reaction time (100 °C for 1 h and 120 °C for 2 h). Selected experiments were carried out in the further presence of SiO_2 pellets (10 $g \cdot L^{-1}$; 0.2÷0.5 mm size). The ultrasonication pre-treatment was performed with an ultrasound probe (Sonoplus HD 4100, Bandelin) immersed in the aqueous algae suspension for 10 minutes at the maximum power. After the treatments, the suspensions were filtered and the concentration of sugars in the filtrate analysed by HPLC.

2.3. Characterization of the Nb-based solid catalysts

Two different heterogeneous catalysts were used in the algae valorisation. They were the commercial powders: HY-340, corresponding to niobic acid, i.e. amorphous hydrated Nb_2O, and therefore labelled in the following as Nb_2O_5, and hydrated nioubim oxyphospate $NbOPO_4$. Both solids were kindly provided from the Companhia Brasileira de Metalurgia e Mineração (CBMM) and they were used as received. An in-depth chemical-physical characterization of the two commercial CBMM catalysts has already been reported several times in the literature [23,24, 28-32], consequently, we have confirmed the characteristics already published and in the present study we report further characterizations, detailed below, to support and enrich the discussion. The specific surface area (SSA) of the samples was measured by using a Micromeritics FlowSorb 2300 apparatus. Scanning electron microscopy (SEM) was carried out using a FEI Quanta 200 ESEM microscope, operating at 20 kV on specimens upon which a thin layer of gold had been evaporated. High-resolution transmission electron microscopy (HRTEM, JEOL-JEM-2100F) and scanning transmission electron microscopy (STEM, Gatan) combined with energy dispersive X-ray spectroscopy (Oxford, EDX) were performed to inspect the structures at high magnification and determine their nanostructure and elemental composition and distribution. Fine powder of every sample was dispersed in ethanol, shortly sonicated, and sprayed on a Lacey-carbon-on-copper grid (200 mesh, EM science), and then allowed to air dry. Then, the dried grid was mounted on a JEOL single-tilt holder. Acquiring, processing and analysis of all micrographs were performed using Gatan Digital Micrograph software. Quantitative analyses were done using INCA Microanalysis software. Vibrational spectroscopies, FTIR and Raman, were used to verify the structural features of the solids. FTIR spectra of the samples in KBr (Aldrich) pellets were obtained by using a FTIR-8400 Shimadzu spectrometer with 4 cm^{-1} resolution and 256 scans and spectra were recorded before and after the reaction to evidence the possible presence of humins. Raman spectra were registered by using a Renishaw in-via Raman spectrometer equipped with an integrated microscope and with a charged-coupled device (CCD)camera. A He/Ne laser operating at 632.8 nm was used as the exciting source. The power of the laser used was 15% of the maximum value that was around 300 mW. Three different measures on the same sample were carried out in different positions on the specimen to confirm the homogeneity and reproducibility of the measure. The quantification of Brønsted acid sites on the surface of the materials was performed in aqueous suspension by the titration method with 0.01 M NaOH (aq) as reported in literature for acidic solids [33]. In a typical experiment, 0.1 g of solid was added to 25 ml of deionized water. The resulting suspension was allowed to equilibrate for 24 hours under stirring and thereafter it was titrated by dropwise addition of 0.01 M aqueous solution of NaOH using phenolphthalein as the neutralization indicator.

2.4. Catalytic reactivity set-up: Hydrothermal conversion of *Chlorella sp*. into furans

The stainless-steel autoclave hydrothermal reactor described in 2.1. was used as catalytic reactor and the reactions proceed by using the same set-up described before. In the PTFE beaker, 24 mL of the pre-treated suspension (see section 2.2), previously filtered through 0.2 μm membranes (CA, Millipore), were placed. The heterogeneous catalytic reactions were carried out in the presence of the commercial Nb_2O_5 or $NbOPO_4$. Other variables were the reaction temperature and time, as well as

the mass ratio catalyst/biomass. The starting of the reaction has been considered the moment in which the autoclave was immersed into the hot oil bath.

Some experiments were performed in the presence of a biphasic system in the contemporary presence of an aqueous suspension and an organic solvent. For that aim, 12 mL of the pre-treated suspension and 12 mL of Methyl IsoButyl Ketone (MIBK) or 4-heptanone were placed into the chamber along with the solid catalyst. A selected experiment was carried out in the presence of 200 mg mL^{-1} of NaCl in order to understand the influence of the ionic strength effect in the conversion and selectivity. After the treatments, aliquots from both the organic and the aqueous phase were filtered and 5-HMF, furfuryl aldehyde and residual sugars concentrations were analysed by means of the HPLC described in 2.1. Results are expressed as yield (Y) to 5-HMF, calculated as follows:

$$Y = \frac{\text{mol HMF}}{\text{mol glucose+mol fructose}} \cdot 100 \quad (1)$$

2.5. Experimental design through (DoE) methodology

The study of the experimental variables involved in the catalytic transformation of sugars into furans was carried out by an experimental design of 20 trials suggested by the Design-Expert 13® (DoE) software. The variables studied were temperature (variable A), between 160°C and 210°C, time of reaction (variable B), between 4.45 and 16 h and percentage of catalyst with respect to the initial biomass (variable C), between 50 and 200%. The model output is the percentage yield to 5-HMF starting from the extracted sugars. A central composite design with the mentioned three inputs and only one output (the obtained concentration of the product 5-HMF) was chosen.

2.6. Calculation of the electric power consumption

A network analyzer was connected to the synthetic oil bath containing the autoclave chamber employed for the catalytic reactions. The analyzer, Frer Nano Mono 63A, was connected to the power line of the heating plate LLG-uniSTIRRER 7 and the recorded data were analysed to quantify the power consumption during the use of the system.

3. Results and discussion

3.1. Effect of pre-treatments on sugars availability

Several kind of pre-treatment on biomass have been reported, and each of them showed different performance depending on the nature of the cell-wall of the algae under study [12]. In particular, microalgae of the genus *Chlorella sp*. are usually equipped of a very resistant cell wall, made of insoluble polymers. The microalga employed in this work is autochthonous and for this reason there are no technologies ready for the degradation of its cell-wall. Consequently, with the aim to release the maximum possible amount of sugars from the cell, employing procedures in which the use of concentrated solutions of inorganic acids is avoided, various pre-treatment methods and conditions test, detailed in Table 1, were carried out. In Table 1 the amount of sugars released during the pre-treatment is reported as a percentage of their total amount, released by using HCl concentrated water solution (see section 2.1), that resulted to be equal to 9.1 mg in 40 mg of lyophilised biomass, corresponding to ca. 22.7 % of the total mass.

Table 1. Experimental conditions applied in the preliminary treatment of *Chlorella sp*. algae along with the percentage of sugars released with respect to their total amount measured by following the procedure described in section 2.1.

Run	Pretreatment	Time [h]	Temperature [°C]	Sugar released [%]
A	Hydrothermal (in H_2O)	1	100	16.9
B	Hydrothermal (in H_2O)	2	120	18.0
C	Hydrothermal (in CH_3COOH 0.1 M)	1	100	20.6
D	Hydrothermal (in CH_3COOH 0.1 M)	2	120	18.4
E	Hydrothermal (in CH_3COOH 0.1 M) in the presence of SiO_2 pellets	2	120	29.5
F	Ultrasonication	10 min	r.t.	24.1
G	Ultrasonication followed by hydrothermal (in H_2O)	10 min and 2 h	r.t. and 120	27.9
H	Ultrasonication followed by hydrothermal (in CH_3COOH 0.1 M) in the presence of SiO_2 pellets	10 min and 2 h	r.t. and 120	35.3

*r.t. stands for room temperature

Pre-treatments were distinguished by the medium in which the hydrothermal treatment have been carried out, i.e., only water or acetic acid diluted aqueous solution. For each of them, two different severity levels were applied, by changing the temperature (100 or 120 °C) and the reaction time (1 h or 2 h). Acetic acid was employed also in the presence of SiO_2, due to the mechanical damage that silica pellets can cause to the cell and due to its acidic nature. As a further treatment, ultrasonication was chosen and applied either alone or followed by a hydrothermal treatment. In experiments G and H, after ultrasonication a hydrothermal treatment in water (G) or in acetic acid solution in the presence of SiO_2 (H) for 2 h at 120 °C was performed.

A perusal of Table 1 evidences that amongst the pre-treatments carried out at 100 °C for 1 h, the presence of acetic acid (experiment C) increased the hydrolysis of the biomass ensuring a release of sugars of 20.6%, while in water alone (A) it was only 16.9%. At 120 °C for 2 h, water hydrolysis (B) and acetic acid mediated hydrolysis (D) gave similar results, i.e. 18 and 18.4%, respectively. When acetic acid was employed in the presence of SiO_2 (E), the release of the sugars was 29.5%. The addition of SiO_2 has a notable effect on the release of sugars probably because it induces an increase in the cell disruption. Although studies showing cytotoxic effect of SiO_2 nanoparticles (10-20 nm) in *Dunaliella tertiolecta* are reported [34], the SiO_2 particles used in this work were bigger (size 200-500 μm) than those of the aforementioned work, and probably they helped in the rupture of the cell membrane due to mechanical stress. In order to increase the percentage of sugar release, we tested an alternative pre-treatment, i.e. ultrasonication homogenisation. The ultrasonication is often employed for the pre-treatment of biomass because ultrasound waves cause the periodical compression and rarefaction when propagating through the medium. Ultrasonication alone (F) caused 24.1% of sugar release; the combination of ultrasonication and successive hydrothermal treatment resulted in 27.9% and 35.3% of sugar release at 120°C for 2 h in water (G) and in acetic acid and SiO_2 (H), respectively. For this reason, we chose to proceed with experiments by using this last pre-treatment (H) as preliminary step of the catalytic reactions.

The ultrasonication and successive hydrothermal treatment releases a quantity of sugars comparable to that reported on recent literature. For example, the employment of pulsed electric field in *Chlorella vulgaris* leads to a carbohydrates yield of 25 to 39% of the total carbohydrate content, the employment

of Ionic Liquid on *Chlorella vulgaris* leads to a carbohydrates yield of 26% of the entire carbohydrate content [35]. An enzymatic pre-treatment on *Chlorella pyrenoidosa* leads to a sugar yield of 19% of biomass [36].

3.2. Characterization of the catalysts

As far as regards the morphological characterization of the catalysts to be used in the isomerisation/dehydration reaction of the released sugars, Figure 3 shows the SEM micrographs of the two catalysts before and after their use in the catalytic tests. Both fresh catalysts consist of agglomerates of nanoparticles ranging in size from 20 to 40 nm in the case of Nb_2O_5, and between 12 and 20 nm for $NbOPO_4$. HRTEM inspection of Nb_2O_5 (Figure 4a,b) and $NbOPO_4$ (Figure 4c,d) confirmed that the agglomerates at the nanoscale do not show any crystallinity and all selected area electron diffraction patterns (see supporting information) were typical of amorphous structures. The STEM-EDX area mapping and quantitative analysis showed the homogenous distribution of Nb and O (Figure 5 upper panel, table 2) and Nb, P and O (Figure 5 lower panel, table 3) in the agglomerates of Nb_2O_5 and $NbOPO_4$, respectively. After the catalytic experiments, an increase in particle size up to 26-40 nm was observed for the $NbOPO_4$ catalyst, indicating a sort of thermal sintering of the particles only in the case of this material. In particular, after the catalytic experiments the particle dimensions of the two catalysts Nb_2O_5 and $NbOPO_4$ were found to be very similar.

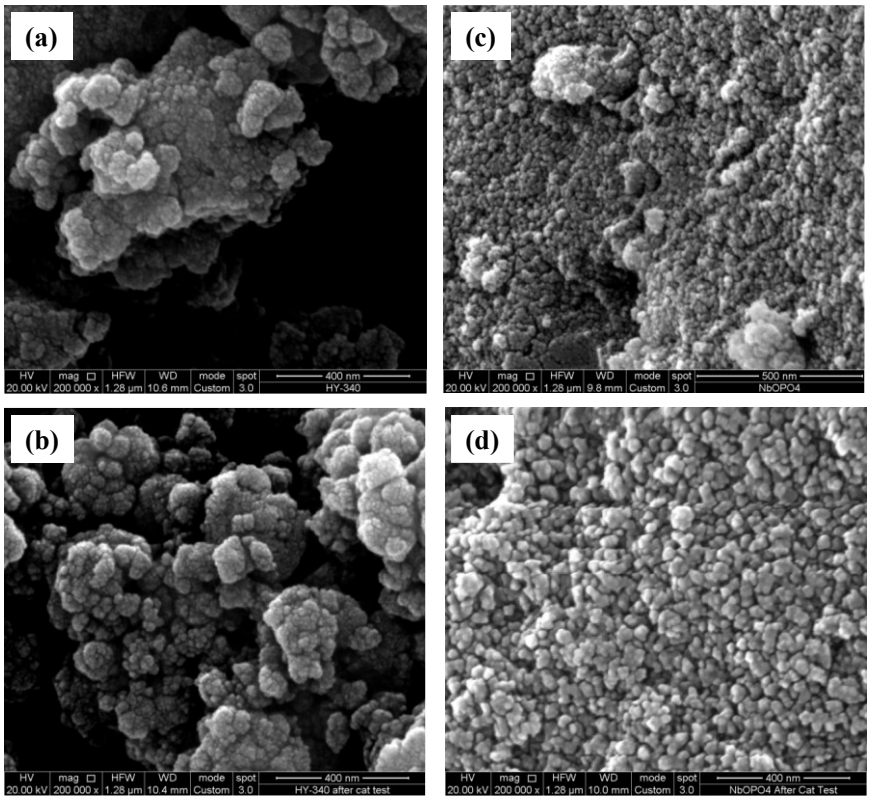

Figure 3: SEM micrographs of the catalysts (a) Nb_2O_5 fresh and (b) after being used in reaction, and (c) $NbOPO_4$ fresh material (d) after being used in the catalytic reaction.

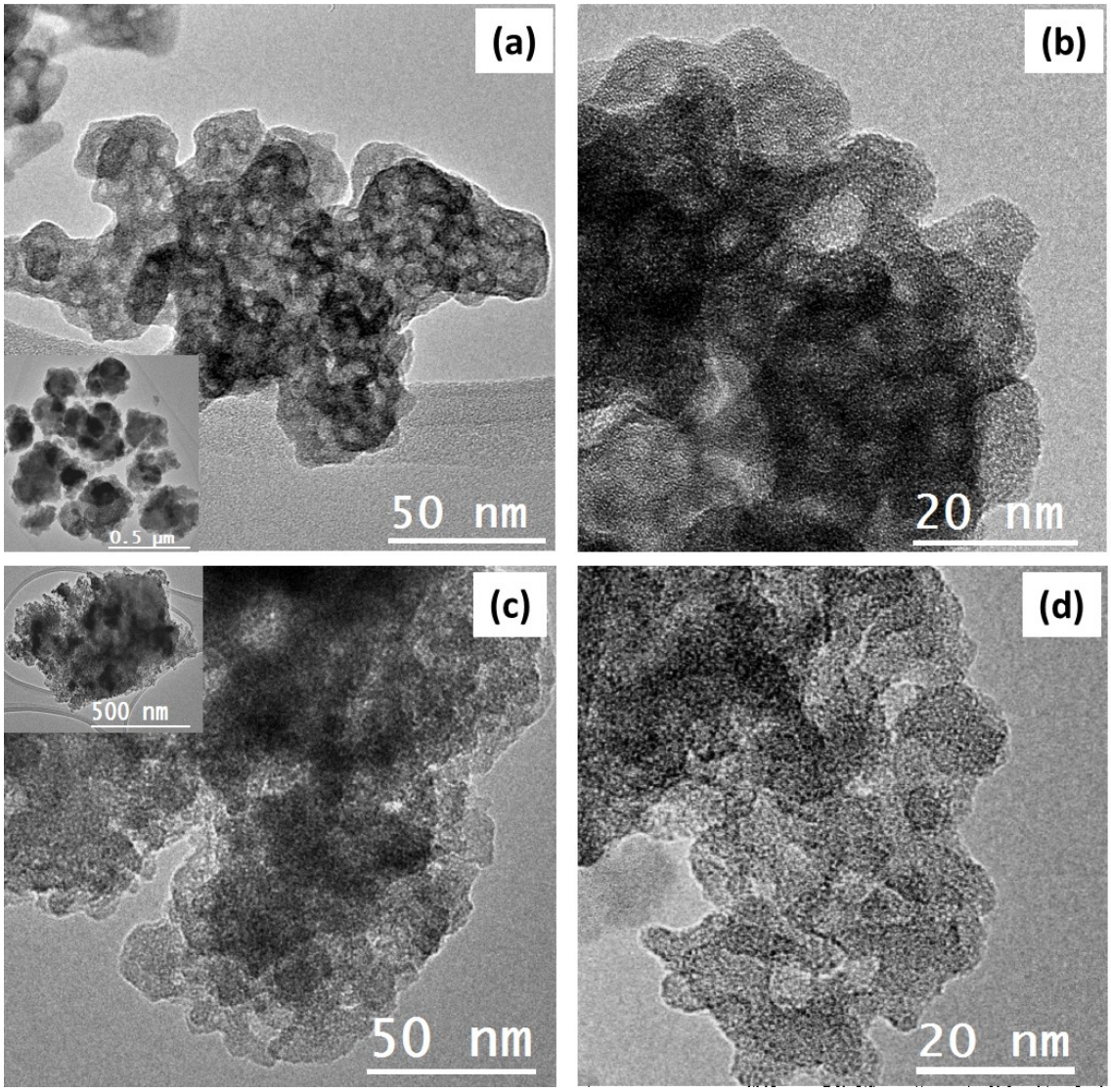

Figure 4. HRTEM imaging of Nb_2O_5 (a,b) and $NbOPO_4$ (c,d) at different magnification scales proving their amorphous structures.

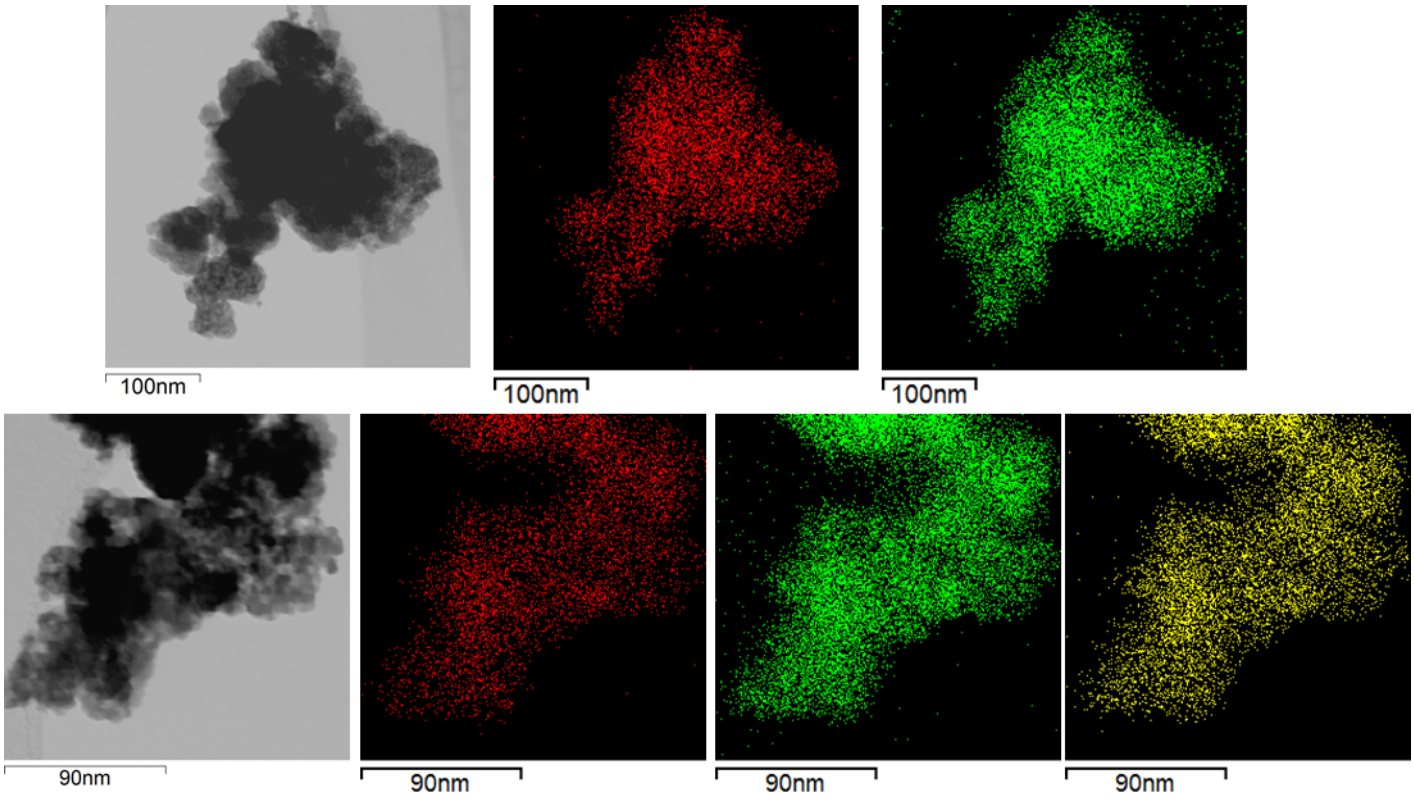

Figure 5. Bright-field STEM imaging (grey scale images) and EDX area mapping for agglomerates of Nb_2O_5 (upper panel) and $NbOPO_4$ (lower panel) for the elements: Niobium (red), Oxygen (green) and phosphorus (yellow) proving the homogenous distribution of all elements at the nanoscale.

Table 2. EDX quantitative analysis showing the normalized atomic % of several Nb_2O_5 agglomerates

Element	Atomic%	Standard deviation
Nb	32.07	1.68
O	67.93	1.68

Table 3. EDX quantitative analysis showing the normalized atomic % of several $NbOPO_4$ agglomerates

Element	Atomic%	Standard deviation
Nb	19.06	1.27
O	69.30	2.11
P	11.64	1.09

The crystallinity of both commercial Nb_2O_5 and $NbOPO_4$ solids has been studied before by XRD [37] evidencing the amorphous character of both powders. FTIR was carried out to study the structure of the samples both as received and also after being used in the catalytic reaction. FTIR spectra of both samples are reported in Figure 6(A). For both samples the typical bands assigned to water are present. The large band centered at ca. 3300 cm^{-1} is attributed both to the hydroxyl groups of the water physically adsorbed on the catalyst surface and to the Nb-OH groups, whereas the transitions at ca. 1680 cm^{-1} is due to the bending of the water. The intense peak at 590 cm^{-1} with a shoulder at 890 cm^{-1} have been assigned to Nb-O groups and Nb=O vibrations, respectively [38]. The $NbOPO_4$ sample furtherly showed a strong transition centered at 1010 cm^{-1}, assigned to the O=P=O asymmetric

stretching vibration of phosphate species [39]. In $NbOPO_4$, the Nb=O stretching frequency is masked by the phosphate vibrations. Interestingly, no apparent differences in the FTIR spectra were observed for the spent catalysts with respect to the original materials, indeed the colour of the used catalysts did not changed significantly with respect to the initial solid. Also Raman spectroscopy has been employed to investigate structure features of both catalysts. Figure 6 (B) shows the Raman spectra related to both solids. Each measurement was performed at different positions on the surface of the specimen in order to verify the homogeneity of the material. Three broad vibrational transitions characterised the Nb_2O_5 spectrum, centered at ca. 660, 200, and 150 $cm^{-1,}$ the most intense at ca. 660 cm^{-1} has been attributed to stretching vibrations of the Nb-O-Nb bridging bond of distorted octahedral polyedra NbO_6, as reported before by Pittman for niobic acid [40]. The amorphous degree of the structure is associated to the presence of distorted NbO_6, NbO_7 and NbO_8 polyhedra justifying the broadening of the ≈660 cm^{-1} centered band. Moreover, the group of weak and broad bands in the low-wavenumber region was assigned to the bending modes of the Nb–O–Nb linkages [41]. The widening of the bands attributed to the bending modes of Nb–O–Nb distorted bridges is justified by the amorphous niobic acid structure. This results are in agreement with the previous observations[37]. The structure of the niobic acid, the HY-340 sample, consists of distorted NbO_6, NbO_7 and NbO_8 polyedra containing also water molecules bonded by hydrogen bonds to the oxygens of various strengths [42]. These hydrated polyedra are responsible for the Brønsted acid centers [43,44]. The Raman spectrum of $NbOPO_4$ is characterised by two main peaks. The strong band present at 680 cm^{-1} can be assigned to the stretching O-Nb-O mode of the distorted NbO_6 polyhedra, whereas the phosphate units, O-P-O bonds, can possess different geometries according to their connectivity depending upon the number of bridging oxygen atoms per PO_4 tetrahedron (n = 0 to 3) [45]. According to Razum et al., the phosphates vibrational transitions are responsible for the group of bands in the range 750 to 1100 cm^{-1}; for instance, the signal at 780 cm^{-1} can be attributed to stretching P-O-P but also to O-Nb-O bonds coupled to O-P-O deformation modes; and the shoulder centered at ca. 925 and 1010 cm^{-1} to the O-P-O the symmetric and asymmetric stretching, respectively. The presence of the above described vibrational transitions justify and support the existence of structures reported in Figure 2 for the catalysts used in this research.

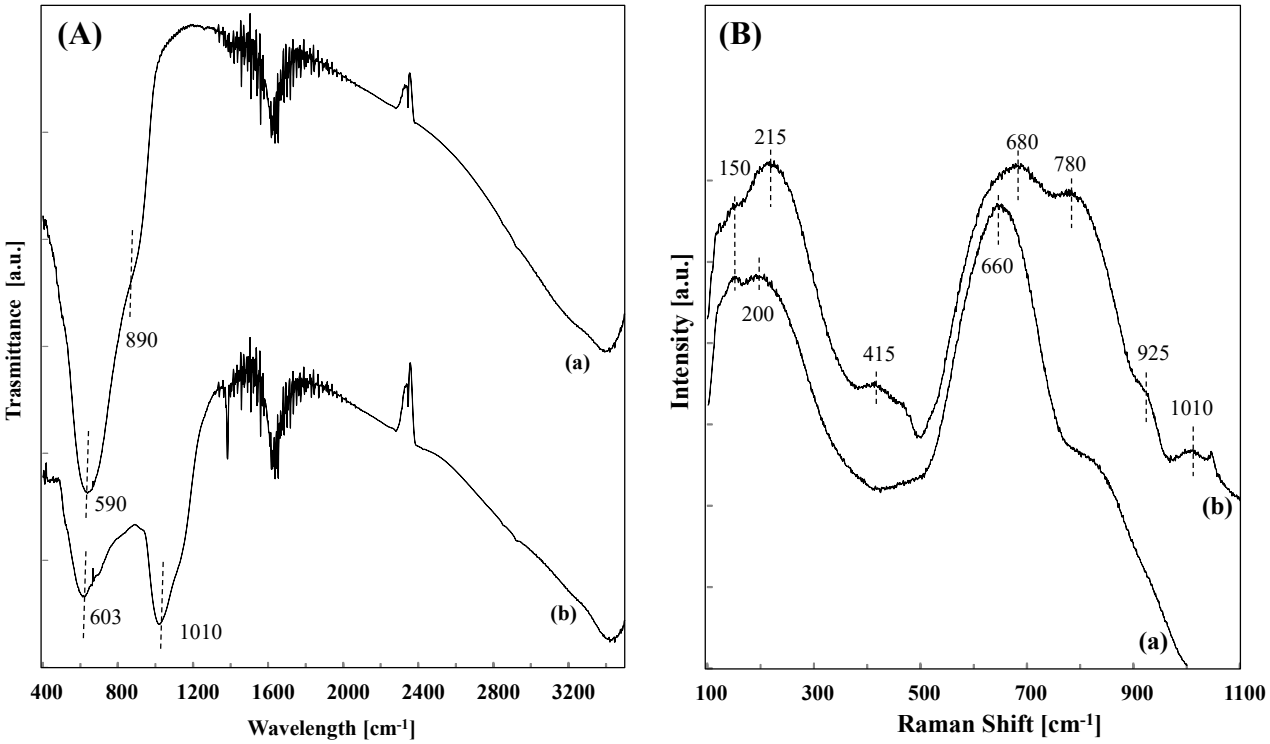

Figure 6. (A) FTIR and (B) Raman spectra of the catalysts (a) Nb_2O_5 and (b) $NbOPO_4$

The results obtained from textural characterization of the samples are shown in Table 4. Both Nb_2O_5 and $NbOPO_4$ catalysts showed similar specific surface areas, nonetheless, according to literature reports, where type IV BET classification adsorption-desorption isotherms have been reported for both solids, $NbOPO_4$ presented higher pore volume and diameter values than Nb_2O_5 [46] attributed to the 2D lamellar structure of $NbOPO_4$ shown in Figure 2 (B), capable of occlude neutral molecules, as water. The acidity of catalysts in aqueous suspension was determined by titration with NaOH. This method quantifies only the Brønsted acid sites through the measurement of free protons in solution due to the initial cation exchange between the catalyst surface and the solvent. The acidity measured by titration evidenced the much higher acidity of $NbOPO_4$ with respect to the niobic acid Nb_2O_5, which can enhance the 5-HMF yield in the monosaccharide isomerisation/dehydration reaction.

Table 4. Specific surface area and acid properties of prepared catalysts as determined by NaOH 0.01 M titration.

Catalyst	Specific surface area [$m^2 \cdot g^{-1}$]	Acid sites by NaOH titration [mmol H^+ g^{-1}]	Surface density of Brønsted acid sites $\times 10^3$ [mmol H^+ m^{-2}]
$NbOPO_4$	119	31.8	270
Nb_2O_5	115	0.694	6.03

3.3. Heterogeneous catalytic valorisation of *Chlorella sp.* in the presence of Nb_2O_5 and modelling of the results

Table 5 shows the results of the catalytic experiments conducted according to the design obtained from the DoE software. The monosaccharides (glucose and fructose) content of the dried *Chlorella sp*, estimated as indicated in Section 2.1, resulted the 22.7% of the total mass for each algal sample. This sugar content was used to determine the yield to 5-HMF by using equation 1. However, in Table

5 is reported also the yield to 5-HMF with respect to the amount of sugars released during the algae pre-treatment.

Table 5. Experimental design based on Design-Expert 13 software applied for the heterogeneous catalytic reactivity and results of the experimental trials. Results are expressed as yield to 5-HMF considering as starting amount of sugars both the total sugars measured in section 2.1 and the extracted sugars after the pre-treatment. All the experiments were carried out by using Nb_2O_5 as the catalyst.

Run	A:Time [h]	B:Temperature [°C]	C: [a]Catalyst [%]	[b]Yield to 5-HMF with respect to total sugar content [%]	[c]Yield to 5-HMF with respect to released sugar [%]
1	4.45	160	50	6	17
2	16.0	160	50	16	45
3	4.45	210	50	15	61
4	16.0	210	50	7	24
5	4.45	160	200	16	38
6	16.0	160	200	21	59
7	4.45	210	200	18	73
8	16.0	210	200	6	21
9	0.5	185	126	0	0
10	20.0	185	126	13	48
11	10.3	143	126	3	11
12	10.3	227	126	9	31
13	10.3	185	0	7	25
14	10.3	185	251	13	47
15	10.3	185	126	17	60
16	10.3	185	126	13	49
17	10.3	185	126	19	60
18	10.3	185	126	13	49
19	10.3	185	126	19	60
20	10.3	185	126	17	60

[a]Percentage of catalyst with respect to the initial biomass; [b]Yield based on the algae total sugars content; [c]Yield based on the algae released sugars during the pre-treatment.

The best yield to 5-HMF, with respect to the released sugar in the pre-treatment, is 73%, corresponding at 18% with respect to the total sugars (run 7). Runs 3, 6, 15 and 20 give also good results with yield to 5-HMF of 61-59% with respect to the released sugar and 15-21% with respect to the total sugars. Since the salt contained in the lyophilized alga (the presence of anions was mainly limited to phosphates (32 ppm) and chlorides (270 ppm)) can affect the conversion of the sugars to 5-HMF, an experiment (not reported) was carried out in the presence of a high amount of NaCl (270 ppm as Cl^-) in a synthetic glucose solution. From this experiment we concluded that the presence of chlorides decreased the glucose conversion but the selectivity to 5-HMF remained almost constant, hence the yield to 5-HMF decreased. Moreover, it was interesting to note that at the same time, the selectivity to fructose increased. These results suggest that the presence of chloride ions not only reduces the glucose conversion, but it is also responsible for reducing the formation of by-products

different from fructose and 5-HMF. Consequently, the presence of salt is not completely undesirable, and then it is not convenient to remove them from the solution. The obtained yields compared to the total sugar content are comparable to what found by other researchers in previous works. For example, Wang et al. obtained a 5-HMF yield from 7.5 to 18.5% from *Chlorococcum sp*. biomass by using H-ZSM-5 zeolite as catalyst at 200 °C for 2 h [47]. Jeong et al. obtained a maximum HMF yield of 22.3% from *Chlorella sp*. with a metal sulphate homogeneous catalyst at 165°C for 30 min [48]. Jeong obtained the maximum 5-HMF yield of 37.23% at 170°C and 60 min from *Chlorella sp*. using a two-step approach in the presence of ferric sulphate as homogeneous catalyst [49]. It is worth noting that the mentioned works report reaction times shorter than those used in the present work. This may be due to the temporal starting point considered, which, in this work, corresponds to the moment in which the autoclave was immersed in the boiling oil. A specific time is required to warm up the entire reactor, which increases the overall reaction time.

The Design Expert software was then employed for analysing the experimental data. The software employs a mathematical model with the aim of fitting in the best possible way the experimental points. The best fitting was obtained by means of a quadratic equation with an F-value of 18.4 and a p-value < 0.0001, which implies that the model is significant, an R^2 of 0.94 and a signal to noise ratio of 14.479. The analysed factors were A- Time, B- Temperature and C- % catalyst. The significant parameters employed by the model were A, B, C, AB, B^2, C^2.

Table 6 reports variables, coefficients together with the relevant F and *p* values. From the analysis of coefficients, it is revealed that the strongest antagonistic effect on the final output is due to the variable AB, while C has the highest synergistic effect.

Table 6: Estimation and statistic of coefficients

Variable	**Coefficient**	**F-value**	**p-value**
Intercept	55.75	18.74	< 0.0001
A-Time	-6.14	10.58	0.0100
B-Temperature	3.88	6.47	0.0315
C-% catalyst	5.97	15.28	0.0036
AB	-17.21	74.39	< 0.0001
AC	-2.58	1.67	0.2288
BC	-3.37	2.85	0.1255
A^2	2.48	1.63	0.2340
B^2	-11.31	55.11	< 0.0001
C^2	-6.12	16.13	0.0030

Figure 7(a) shows the predicted values vs the actual results of the trials. Line represents perfect model performance; the model offers therefore a very good fitting. The 3D surface of percentage yield starting from extracted sugars is shown in Figure 7(b). The response of the model is reported in terms of Yield (%), shown in z-axis, vs Time (h) and Temperature (°C), shown respectively in x and y axis. In figure 7, the modelling with 200% of catalyst with respect to the initial biomass is shown. For lower amount of catalyst the 3D surface presents the same shape but with yield values shifted downward.

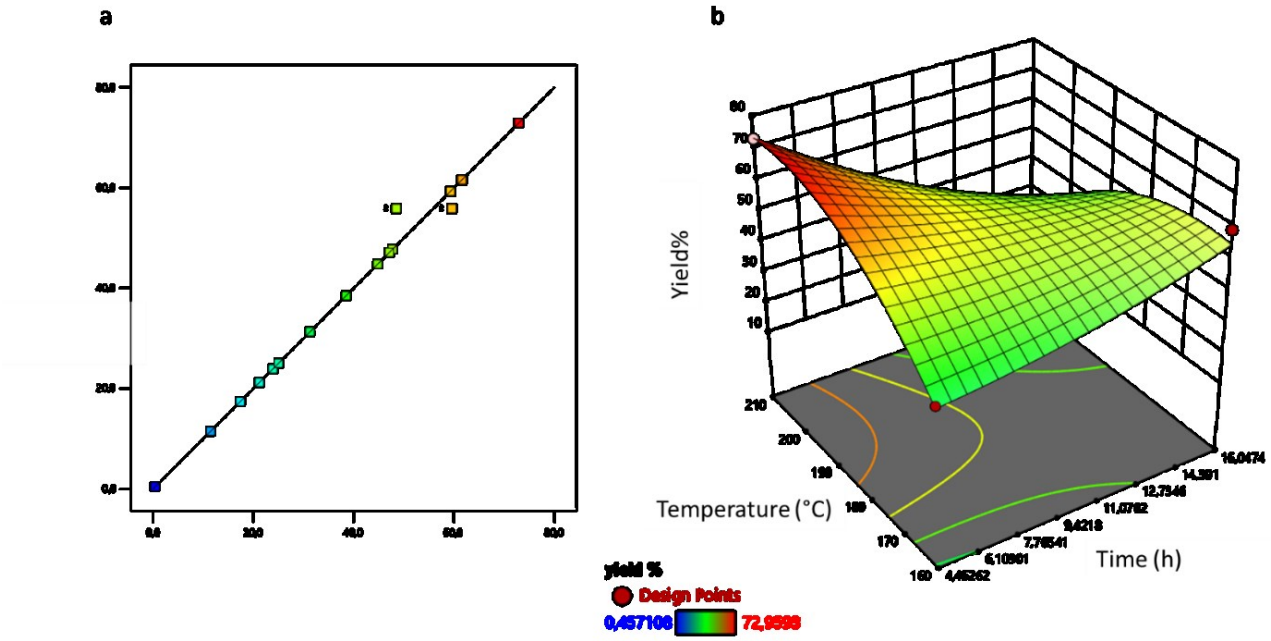

Figure 7. (a) Model prediction vs actual results of the trials expressed as Yield based on the algae released sugars during the pre-treatment (b) response surface of the % yield as a function of Temperature and Time with 200% of catalyst with respect to the initial biomass. Colours of points determine the yield percentage to 5-HMF in the experimental responses.

According to the model prediction, in order to achieve optimal yields to 5-HMF, both time and temperature need to be carefully adjusted. When high temperatures are chosen, a relatively short reaction time is optimal, conversely, at low temperature long reaction time is needed. This occurs because, as well known and schematised in Figure 1, 5-HMF in water may polymerize together with other products and sugars to form humins, as side polycondensation product [50,51]. The formation of humins is favoured by increasing the initial concentration of its precursors; for this reason, when protracting the reaction for more than 4.45 hours at high temperature (210 °C) the model predicts a decrease of the yield to 5-HMF. On the other hand, the acidic catalyst role enhances the concentration of 5-HMF for the highest tested concentrations (200 % with respect to the initial biomass). The heterogeneous catalyst does not interfere with the effect of time and temperature, but simply increases the yields under all the conditions.

In literature, simple models have been proposed for the conversions of glucose/fructose or cellobiose to 5-HMF in the presence solid catalysts [52-54]. It is well known that the conversion of glucose/fructose to 5-HMF follows the steps: (1) glucose isomerization to fructose, (2) fructose dehydration to 5-HMF, and (3) 5-HMF rehydration to levulinic acid (LA) and formic acid (FA) (See Figure 1). This last step accounts for the decreasing of 5-HMF yield after a certain reaction time, as predicted by our model: 5-HMF may disappear due to the formation of humins but also for its rehydration to form LA and FA.

Wang et al. concluded that for the conversion of glucose to 5-HMF in the presence of a homogeneous catalyst such as LiCl, the reaction temperature had an important impact on the activity, confirming

the results of the present research. Analogously to our present work, Ramli et al., in heterogeneous catalytic regime in the presence of a Fe/HY zeolite catalyst, conclude that in the conversion of glucose to 5-HMF the reaction rate increased by enhancing the temperature.
A multiparameter statistical approach was employed previously for the optimization of microalgal conversion in 5-HMF [43,44,50]. They found as best fitting, a quadratic equation for the modelling 5-HMF production from *Chlorella sp*. using as parameters temperature, catalyst concentration and reaction time with a similar approach to this work [48]. Their results are apparently contrasting to what we have found here, but this may depend again on the chosen experimental conditions for the time equal to zero. Alternatively, it may be possible that the sugars were more available for conversion than in our system, therefore shorter times and lower temperatures were required. In another work, the same author employed the same quadratic equation for the modelling of 5-HMF production from *Chlorella sp*. using as parameters temperature, catalyst concentration and reaction time [49]. In this last work, carried out in the presence of a solubilised salt, $Fe_2(SO_4)_3$, as catalyst, low temperatures (140 and 150 °C) and longer times were necessary for the conversion to 5-HMF while at higher temperature (190°C), shorter times were needed, similarly to what found in the current research. The lower duration of the overall reactions could be attributed to differences with respect to us in the consideration of the zero time of reaction, and/or because of the use of an homogeneous catalyst instead of a solid one. Instead, other authors have found a quadratic equation as best fitting for the modelling of 5-HMF production from *Chamydomonas reinhardtii* using as parameters DMSO %, H_2SO_4% and temperature [55].
Our results suggested that the best catalytic performance in the presence of Nb_2O_5 is provided from reactions conducted at high temperature (210 °C) for short time (4.45 h) or at low temperature (160 °C) for long reaction time (16 h). In order to better evaluate the two conditions, we measured the energetic consumption in our system in the two conditions. Results indicated that at 160 °C for 16 h the system consumed 4.53 KWh, while at 210 °C for 4.45 h the consumption was 1.56 KWh. For this reason, in the subsequent experiments these last conditions were preferred and employed as control. All further results will be expressed as a percentage of this value.

3.4. Optimization through $NbOPO_4$ catalyst and ketonic solvent reactive extraction

With the aim of optimising the reaction yield to 5-HMF, in the light of the results obtained by the hydroxide titration of the acidic surface of Nb_2O_5 and $NbOPO_4$, as well as considering the literature reports, also niobium oxyphosphate, $NbOPO_4$ was used as heterogeneous catalysts for the isomerisation/dehydration of the sugars released by the algae. The results achieved by using this last catalyst are reported in Figure 8 and are expressed as percentage of the yield to 5-HMF obtained in the control run, conducted at 210 °C for 4.45 h in the presence of Nb_2O_5·catalyst. Using the $NbOPO_4$ catalyst under the same conditions as in the optimized experiment (control test) increases the 5-HMF yield by 17.4%. This outcome was expected, considering the slightly higher specific surface area but mainly the remarkable enhanced overall acidity in aqueous suspension of the oxyphosphate with respect to the niobic acid (see Table 4). The alternative optimized conditions identified by the DoE approach were also tested, i.e. by decreasing the temperature from 210 °C to 160 °C, increasing reaction time from 4.45 h to 6 h and a combination of the two, but the yield was decreased by 82.1, 5.1 and 77.4%, respectively, compared to the control test. These results suggest that the optimum reaction conditions to isomerise/dehydrate the monosaccharides obtained from the step 1 in the

presence of $NbOPO_4$ appears to be 210°C for 4.45 h, probably because the ratio Brønsted and Lewis acid sites of Nb_2O_5 and $NOPO_4$ is different.

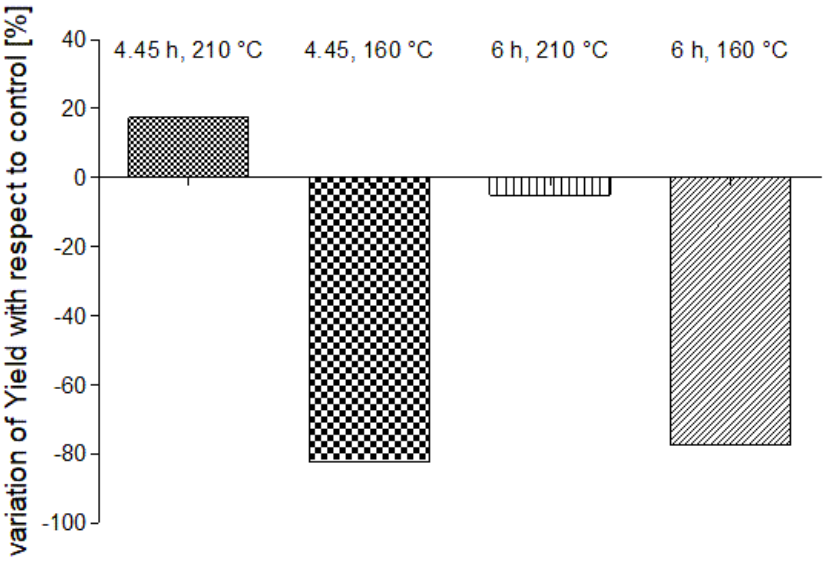

Figure 8. Percentage of increase (positive value) or decrease (negative values) of the yield to 5-HMF with respect to the value obtained in the control test for experiments carried out at different time and temperature by using $NbOPO_4 \cdot nH_2O$ as the catalyst.

Several studies have been reported on the fructose and/or glucose dehydration to get 5-HMF in the presence of $NbOPO_4$ in which the use of fructose was favourable than the use of glucose to yield 5-HMF. The higher number of Brønsted acidic sites (BASs) on the oxyphosphate catalyst surface with respect to the oxide has been claimed to justify this finding [20] because Brønsted sites are considered more active for dehydration whereas Lewis sites for isomerisation of glucose to fructose [23]. Indeed, according to literature, the Brønsted acid sites are present in higher amount on $NbOPO_4$ than on the Nb_2O_5 whose Brønsted acid sites present low activity in the dehydration of the hexoses to HMF, which is obtained with low selectivity [56] Considering that both the hydrolysis of polysaccharides to monosaccharides and the dehydration of fructose to 5-HMF are mainly catalysed by BASs [57], the increased yield to 5-HMF in the presence of oxyphosphate catalyst can be attributed to the improvement in both these two steps of the overall process of conversion to 5-HMF, depicted in the introduction (see Figure 1). Apart for the conversion of cellulose to levulinic acid [58] and of industrial syrup to 5-HMF [59], to the best of our knowledge, niobium oxyphosphate has been never used before for the valorisation of biomass and in particular of microalgae to 5-HMF.

With the aim to furtherly increase the yield to 5-HMF, the catalytic sugars conversion was carried out in a reactive extraction system. Two water/organic solvent (50/50 v/v), i.e. H_2O/MIBK and H_2O/4-heptanone, systems were tested in different conditions. MIBK was chosen because it is stable in acidic medium and possesses quite low solubility in water, making it useful for liquid-liquid extraction. Several examples of its employment are reported in literature for both the extraction of sugars from biomass and for the extractive reaction to get 5-HMF [60]. Selected experiments were also carried out in the presence of 4-heptanone, instead of MIBK. 4-heptanone was chosen because according to published theoretical computational analysis taking into account the partition coefficient, water miscibility, boiling point and toxicity of various organic solvents, it resulted the most indicated for this scope [61].

As shown in Figure 9(a), the catalytic dehydration experiment in the presence of Nb_2O_5 carried out for 4.45 h with H_2O/MIBK biphasic solvent, lead to an increase of 30.2% in the yield to 5-HMF with

respect to the control test. This yield increased twice, reaching a 60.6%, by using $NbOPO_4$ as catalysts instead of Nb_2O_5 at the same experimental conditions, leading to a yield compared to the total sugar of the 29%. When the reaction was conducted in the H_2O/MIBK biphasic system for 6 h in the presence of Nb_2O_5, the yield to 5-HMF decreased by 2.05% compared to the control, while for the test carried out 6 h in the presence of $NbOPO_4$ and MIBK the yield increased by 25.4%.

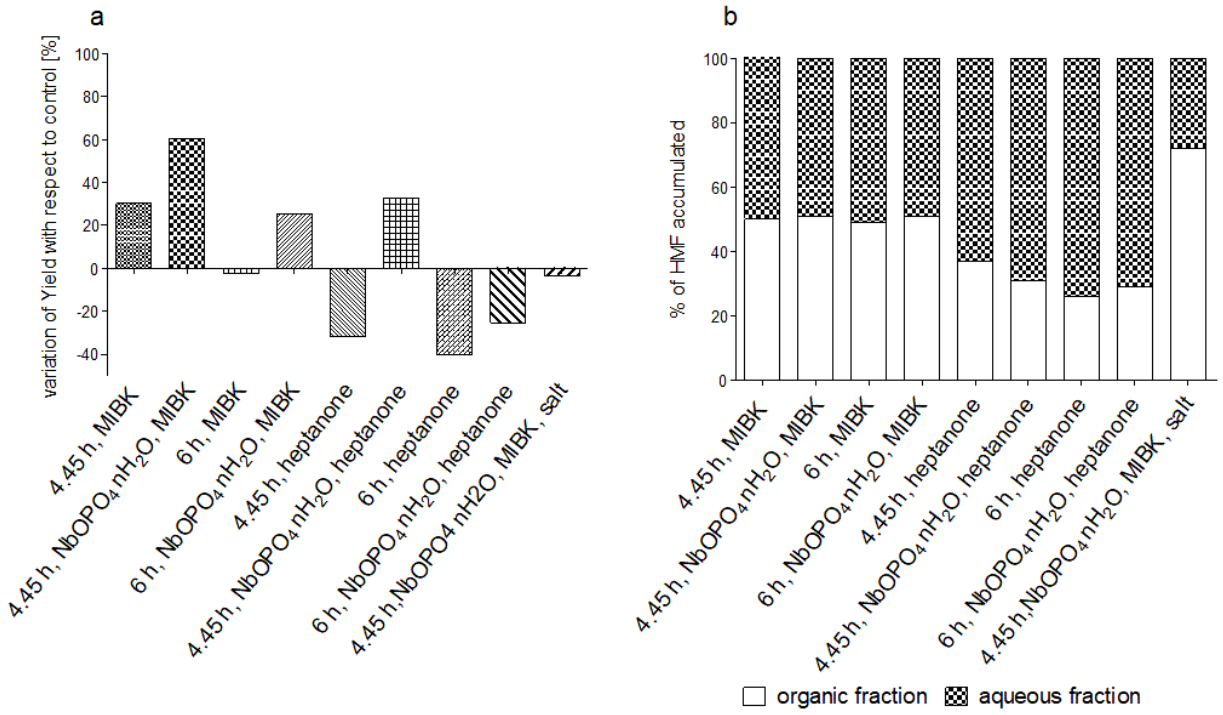

Figure 9: a) Optimization of the overall reaction yield with the use of a biphasic reactive extraction system with two different solvents in different conditions b) Repartition of the products between the organic and the aqueous fractions of the biphasic reactions.

The repartition of 5-HMF between the organic and the aqueous phase is reported in Figure 9(b). When MIBK was used, the repartition was around 50% between the two phases, whereas the 4-heptanone always lead to a decrease of the overall yield, except when it was used in the presence of $NbOPO_4$ in the run lasted 4.45 h achieving a yield 32.6% higher than that achieved in the control experiment. Moreover, 4-heptanone, is less efficient with respect to MIBK to extract 5-HMF from water; indeed, the repartition of the product in the organic phase ranged between 26 to 37% (Figure 9 b).

As already reported in literature, the significant increase in the overall reaction yield when using MIBK as extractive solvent is attributed to a certain solubilisation of 5-HMF in the organic solvent so decreasing its concentration in the aqueous phase and hence the further formation of side-products. In the biphasic reaction systems, the reaction occurs in the aqueous phase, since sugars have low solubility in the organic solvent and also because the solid catalyst is dispersed only in the aqueous phase. Consequently, while the reaction proceeds the product is partially subtracted from the aqueous solution to the organic phase. This leads to enhance both selectivity and yields to 5-HMF when employing MIBK as co-solvent, facilitating at the same time the reusability of the reactive phase with used catalyst [60]. Furthermore, the use of the biphasic system helps the future recovery of the product, lowering the costs for its separation [62,63]. Conversely, the use of 7-heptanone for the

biphasic reaction resulted not convenient, probably because this solvent is not likely to extract 5-HMF and furthermore hinders the advancement of the reaction. This means that the choice of the appropriate solvent is of central importance for the process outcome. Biphasic systems with MIBK solvents were previously applied in the catalytic transformation of cellulose to 5-HMF with good results [64-66], and in some cases for the real biomasses to 5-HMF process [67,68]. As suggested by previous experimentations [63–65], the salting-out effect was studied in the biphasic system with the addition of 200 mg mL^{-1} of NaCl with MIBK solvent and niobium phosphate catalyst. The condition led to a reaction yield almost equal to the control (only 3.3% less). Otherwise, the repartition of the product in the organic fraction was increased compared to the use of MIBK without salt, from 50% to 72%. This should be an advantage from a process point of view. Although a positive effect on overall 5-HMF yield is generally observed in other works [69-71], here, a marked decrease compared to the same condition without NaCl is observed. This difference, anyway, was also observed in other experiments (not yet published) in which the reactivity of niobium oxide catalyst in transforming glucose was decreased by conducting the reaction in presence of ammonium chloride. These results show that the *Chlorella* microalgal recalcitrant biomass may be valorised in 5-HMF with niobium phosphate catalyst in biphasic systems in a biorefinery perspective.

4. Conclusions

A catalytic valorisation of *Chlorella sp* biomass to obtain 5-HMF has been performed and optimised. The reaction has been carried out in two steps; the first one was aimed to extract the carbohydrates from the algae and the second to obtain 5-HMF, by means of a catalytic isomerisation/dehydration, from the extracted carbohydrates. Some procedures were tested to extract the carbohydrates from the algae, but the use of ultrasonication and successive hydrothermal treatment in acetic acid solution gave the best result. The successive steps, isomerisation and dehydration of the carbohydrates extracted from the algae to obtain 5-HMF, were performed by heterogeneous catalysis in hydrothermal conditions. $Nb_2O_5 \cdot nH_2O$ catalyst was used to identify, through a DoE approach, the best reaction conditions, that were 4.45 h at 210°C with 200 % of catalyst with respect to the lyophilized alga. These conditions were further optimised through the use of $NbOPO_4 \cdot nH_2O$ as catalyst and with the adoption of a biphasic system H_2O/MIBK. The partition of the HMF between the aqueous and organic phase was improved by the addition of salt to the aqueous phase. Therefore, in this work, an early-stage process for the transformation of recalcitrant microalgal biomass is proposed.

Declaration of Competing Interest

The authors declare that they have no known competing financial interests or personal relationships that could have appeared to influence the work reported in this paper.

Acknowledgments

This work was carried out with the co-funding of European Union, European Social Fund – REACT EU, PON Ricerca e Innovazione 2014-2020, Azione IV.4 “Dottorati e contratti di ricerca su tematiche dell'innovazione” and Azione IV.6 “Contratti di ricerca su tematiche Green” (DM 1062/2021).

References

[1] S. Lima, P.S.C. Schulze, L.M. Schüler, R. Rautenberger, D. Morales-Sánchez, T.F. Santos, H. Pereira, J.C.S. Varela, F. Scargiali, R.H. Wijffels, V. Kiron, Flashing light emitting diodes (LEDs) induce proteins, polyunsaturated fatty acids and pigments in three microalgae, J. Biotechnol. 325 (2021) 15–24. https://doi.org/10.1016/j.jbiotec.2020.11.019.

[2] R. Arena, S. Lima, V. Villanova, N. Moukri, E. Curcuraci, C. Messina, A. Santulli, F. Scargiali, Cultivation and biochemical characterization of isolated Sicilian microalgal species in salt and temperature stress conditions, Algal Res. 59 (2021) 102430. https://doi.org/10.1016/j.algal.2021.102430.

[3] S. Lima, N. D'Agostino, A. Brucato, G. Caputo, F. Grisafi, F. Scargiali, Civil Wastewater Remediation through Employment of Indigenous Microalgae and Sewage Sludge, Chem. Eng. Trans. 93 (2022) 301–306. https://doi.org/10.3303/CET2293051.

[4] E. Spennati, A.A. Casazza, A. Converti, M.P. Padula, F. Dehghani, P. Perego, P. Valtchev, Winery waste valorisation as microalgae culture medium: A step forward for food circular economy, Sep. Purif. Technol. 293 (2022) 121088. https://doi.org/10.1016/j.seppur.2022.121088.

[5] G.P. 't Lam, M.H. Vermuë, M.H.M. Eppink, R.H. Wijffels, C. van den Berg, Multi-Product Microalgae Biorefineries: From Concept Towards Reality, Trends Biotechnol. 36 (2018) 216–227. https://doi.org/10.1016/j.tibtech.2017.10.011.

[6] E.J. Olguín, G. Sánchez-Galván, I.I. Arias-Olguín, F.J. Melo, R.E. González-Portela, L. Cruz, R. De Philippis, A. Adessi, Microalgae-Based Biorefineries: Challenges and Future Trends to Produce Carbohydrate Enriched Biomass, High-Added Value Products and Bioactive Compounds, Biology (Basel). 11 (2022). https://doi.org/10.3390/biology11081146.

[7] A. Bose, R. O'Shea, R. Lin, A. Long, K. Rajendran, D. Wall, S. De, J.D. Murphy, The marginal abatement cost of co-producing biomethane, food and biofertiliser in a circular economy system, Renew. Sustain. Energy Rev. 169 (2022). https://doi.org/10.1016/j.rser.2022.112946.

[8] J.C.A. Braun, L.M. Colla, Use of Microalgae for the Development of Biofertilizers and Biostimulants, Bioenergy Res. (2022) 289–310. https://doi.org/10.1007/s12155-022-10456-8.

[9] S.S. Siwal, Q. Zhang, N. Devi, A.K. Saini, V. Saini, B. Pareek, S. Gaidukovs, V.K. Thakur, Recovery processes of sustainable energy using different biomass and wastes, Renew. Sustain. Energy Rev. 150 (2021) 111483. https://doi.org/10.1016/j.rser.2021.111483.

[10] N. Zhou, Y. Zhang, X. Wu, X. Gong, Q. Wang, Hydrolysis of Chlorella biomass for fermentable sugars in the presence of HCl and MgCl 2, Bioresour. Technol. 102 (2011) 10158–10161. https://doi.org/10.1016/j.biortech.2011.08.051.

[11] Y. Nemcova, Detection of cell wall structural polysaccharides by cellulase-gold and chitinase-gold complexes, Czech Phycol. (2003) 31–36.

[12] P.S. Corrêa, W.G. Morais Júnior, A.A. Martins, N.S. Caetano, T.M. Mata, Microalgae biomolecules: Extraction, separation and purification methods, Processes. 9 (2021) 1–40. https://doi.org/10.3390/pr9010010.

[13] Y. Zhang, Z. Ding, M. Shahadat Hossain, R. Maurya, Y. Yang, V. Singh, D. Kumar, E.-S. Salama, X. Sun, R. Sindhu, P. Binod, Z. Zhang, M. Kumar Awasthi, Recent advances in lignocellulosic and algal biomass pretreatment and its biorefinery approaches for biochemicals and bioenergy conversion, Bioresour. Technol. 367 (2023) 128281. https://doi.org/10.1016/j.biortech.2022.128281.

[14] R.-J. van Putten, J.C. van der Waal, E. de Jong, C.B. Rasrendra, H.J. Heeres, J.G. de Vries, Hydroxymethylfurfural, A Versatile Platform Chemical Made from Renewable Resources, Chem. Rev. 113 (2013) 1499–1597. https://doi.org/10.1021/cr300182k.

[15] H. Xu, X. Li, W. Hu, L. Lu, J. Chen, Y. Zhu, H. Zhou, C. Si, Recent advances on solid acid

catalyic systems for production of 5-Hydroxymethylfurfural from biomass derivatives, Fuel Process. Technol. 234 (2022) 107338. https://doi.org/10.1016/j.fuproc.2022.107338.

[16] D. Soukup-Carne, X. Fan, J. Esteban, An overview and analysis of the thermodynamic and kinetic models used in the production of 5-hydroxymethylfurfural and furfural, Chem. Eng. J. 442 (2022) 136313. https://doi.org/10.1016/j.cej.2022.136313.

[17] E.I. García-López, F.R. Pomilla, B. Megna, M.L. Testa, L.F. Liotta, G. Marcì, Catalytic dehydration of fructose to 5-hydroxymethylfurfural in aqueous medium over nb2o5-based catalysts, Nanomaterials. 11 (2021). https://doi.org/10.3390/nano11071821.

[18] I. Nowak, M. Ziolek, Niobium Compounds: Preparation, Characterization, and Application in Heterogeneous Catalysis, Chem. Rev. 99 (1999) 3603–3624. https://doi.org/10.1021/cr9800208.

[19] E.I. Ko, J.G. Weissman, Structures of niobium pentoxide and their implications on chemical behavior, Catal. Today. 8 (1990) 27–36. https://doi.org/10.1016/0920-5861(90)87005-N.

[20] M.N. Catrinck, E.S. Ribeiro, R.S. Monteiro, R.M. Ribas, M.H.P. Barbosa, R.F. Teófilo, Direct conversion of glucose to 5-hydroxymethylfurfural using a mixture of niobic acid and niobium phosphate as a solid acid catalyst, Fuel. 210 (2017) 67–74. https://doi.org/10.1016/j.fuel.2017.08.035.

[21] L. Moreno-Real, E.R. Losilla, M.A.G. Aranda, M. Martínez-Lara, S. Bruque, M. Gabás, A Peroxoniobium Phosphate Derived from $NbOPO_4 \cdot 3H_2O$, J. Solid State Chem. 137 (1998) 289–294. https://doi.org/10.1006/jssc.1997.7738.

[22] P. Carniti, A. Gervasini, F. Bossola, V. Dal Santo, Cooperative action of Brønsted and Lewis acid sites of niobium phosphate catalysts for cellobiose conversion in water, Appl. Catal. B Environ. 193 (2016) 93–102. https://doi.org/10.1016/j.apcatb.2016.04.012.

[23] J.L. Vieira, G. Paul, G.D. Iga, N.M. Cabral, J.M.C. Bueno, C. Bisio, J.M.R. Gallo, Niobium phosphates as bifunctional catalysts for the conversion of biomass-derived monosaccharides, Appl. Catal. A Gen. 617 (2021) 118099. https://doi.org/10.1016/j.apcata.2021.118099.

[24] P. Carniti, A. Gervasini, S. Biella, A. Auroux, Niobic acid and niobium phosphate as highly acidic viable catalysts in aqueous medium: Fructose dehydration reaction, Catal. Today. 118 (2006) 373–378. https://doi.org/10.1016/j.cattod.2006.07.024.

[25] A. Florentino, P. Cartraud, P. Magnoux, M. Guisnet, Textural, acidic and catalytic properties of niobium phosphate and of niobium oxide. Influence of the pretreatment temperature, Appl. Catal. A, Gen. 89 (1992) 143–153. https://doi.org/10.1016/0926-860X(92)80229-6.

[26] L. Yan, L. Li, Y. Zhou, C. Hu, C. Lu, X. Shen, Mechanistic kinetic comparison of terrestrial biomass-derived cellulose and marine algae-derived agarose acidic degradation to monosaccharides and 5-hydroxymethylfurfural, Biomass Convers. Biorefinery. (2022). https://doi.org/10.1007/s13399-022-02607-w.

[27] S. Lima, V. Villanova, F. Grisafi, G. Caputo, A. Brucato, F. Scargiali, Autochthonous microalgae grown in municipal wastewaters as a tool for effectively removing nitrogen and phosphorous, J. Water Process Eng. 38 (2020) 101647. https://doi.org/10.1016/j.jwpe.2020.101647.

[28] D. Ma, S. Lu, X. Liu, Y. Guo, Y. Wang, Depolymerization and hydrodeoxygenation of lignin to aromatic hydrocarbons with a Ru catalyst on a variety of Nb-based supports, Chin. J. Catal. 40 (2019) 609-617.

[29] M.M. de Jesus Junior, S.A. Fernandes, E. Borges, B.E. Lôbo Baêta, F. de Ávila Rodrigues, Kinetic study of the conversion of glucose to 5-hydroxymethylfurfural using niobium phosphate, Mol. Catal. 518 (2022) 112079,

[30] P. Magalhães de Souza, L. Alves de Sousa, F. Bellot Noronha, R. Wojcieszak Dehydration of levoglucosan to levoglucosenone over solid acid catalysts. Tuning the product distribution by changing the acid properties of the catalysts, Mol. Catal. 529 (2022) 112564

[31] K.M.A. Santos, E.M. Albuquerque, L.E.P. Borges, M.A. Fraga, Discussing Lewis and Brønsted acidity on continuous pyruvaldehyde Cannizzaro reaction to lactic acid over solid catalysts, Mol. Catal. 458 (2018) 198–205.

[32] J.A. Santana Junior, W.S. Carvalho, C.H. Ataíde, Catalytic effect of ZSM-5 zeolite and HY-340 niobic acid on the pyrolysis of industrial kraft lignins, Ind. Crops Products 111 (2018) 126-132

[33] L.M. Yang, Y.J. Wang, G.S. Luo, Y.Y. Dai, Functionalization of SBA-15 mesoporous silica with thiol or sulfonic acid groups under the crystallization conditions, Microporous Mesoporous Mater. 84 (2005) 275–282. https://doi.org/10.1016/j.micromeso.2005.05.037.

[34] S. Schiavo, M. Oliviero, M. Miglietta, G. Rametta, S. Manzo, Genotoxic and cytotoxic effects of ZnO nanoparticles for Dunaliella tertiolecta and comparison with SiO2 and TiO2 effects at population growth inhibition levels, Sci. Total Environ. 550 (2016) 619–627. https://doi.org/10.1016/j.scitotenv.2016.01.135.

[35] T.Q. To, K. Procter, B.A. Simmons, S. Subashchandrabose, R. Atkin, Low cost ionic liquid-water mixtures for effective extraction of carbohydrate and lipid from algae, Faraday Discuss. 206 (2018) 93–112. https://doi.org/10.1039/c7fd00158d.

[36] S. Bhushan, M.S. Rana, M. Bhandari, A.K. Sharma, H. Simsek, S.K. Prajapati, Enzymatic pretreatment of algal biomass has different optimal conditions for biogas and bioethanol routes, Chemosphere. 284 (2021) 131264. https://doi.org/10.1016/j.chemosphere.2021.131264.

[37] A.M. Barrios, C.A. Teles, P.M. de Souza, R.C. Rabelo-Neto, G. Jacobs, B.H. Davis, L.E.P. Borges, F.B. Noronha, Hydrodeoxygenation of phenol over niobia supported Pd catalyst, Catal. Today. 302 (2018) 115–124. https://doi.org/10.1016/j.cattod.2017.03.034.

[38] L.K.S. Herval, D. Von Dreifus, A.C. Rabelo, A.D. Rodrigues, E.C. Pereira, Y.G. Gobato, A.J.A. De Oliveira, M.P.F. De Godoy, The role of defects on the structural and magnetic properties of Nb2O5, J. Alloys Compd. 653 (2015) 358–362. https://doi.org/10.1016/j.jallcom.2015.09.019.

[39] G.S. Rao, N.P. Rajan, V. Pavankumar, K.V.R. Chary, Vapour phase dehydration of glycerol to acrolein over NbOPO4 catalysts, J. Chem. Technol. Biotechnol. 89 (2014) 1890–1897. https://doi.org/10.1002/JCTB.4273.

[40] R.M. Pittman, A.T. Bell, Raman studies of the structure of niobium oxide/titanium oxide (Nb_2O_5.TiO_2), J. Phys. Chem. 97 (1993) 12178–12185. https://doi.org/10.1021/j100149a013.

[41] K. Nakamoto, Infrared and Raman Spectra of Inorganic and Coordination Compounds, Wiley, 2008. https://doi.org/10.1002/9780470405840.

[42] K. Yoshimura, T. Miki, S. Iwama, S. Tanemura, Characterization of niobium oxide electrochromic thin films prepared by reactive d.c. magnetron sputtering, Thin Solid Films. 281–282 (1996) 235–238. https://doi.org/10.1016/0040-6090(96)08640-3.

[43] Q. Zhang, X. Liu, T. Yang, Q. Pu, C. Yue, S. Zhang, Y. Zhang, Catalytic Transfer of Fructose

to 5-Hydroxymethylfurfural over Bimetal Oxide Catalysts, Int. J. Chem. Eng. 2019 (2019) 1–6. https://doi.org/10.1155/2019/3890298.

[44] J.M. Jehng, I.E. Wachs, Structural chemistry and Raman spectra of niobium oxides, Chem. Mater. 3 (1991) 100–107. https://doi.org/10.1021/cm00013a025.

[45] M. Razum, L. Pavić, L. Ghussn, A. Moguš-Milanković, A. Šantić, Transport of potassium ions in niobium phosphate glasses, J. Am. Ceram. Soc. 104 (2021) 4669–4678. https://doi.org/10.1111/JACE.17882.

[46] F.M. Reguera, L.R.R. de Araujo, M.C. Picardo, F. de O. Bello, C.F. Scofield, N.M.R. Pastura, W. de A. Gonzalez, The use of niobium based catalysts for liquid fuel production, Mater. Res. 7 (2004) 343–348. https://doi.org/10.1590/S1516-14392004000200021.

[47] J.J. Wang, Z.C. Tan, C.C. Zhu, G. Miao, L.Z. Kong, Y.H. Sun, One-pot catalytic conversion of microalgae (Chlorococcum sp.) into 5-hydroxymethylfurfural over the commercial H-ZSM-5 zeolite, Green Chem. 18 (2016) 452–460. https://doi.org/10.1039/C5GC01850A.

[48] G.T. Jeong, S.K. Kim, Hydrothermal conversion of microalgae Chlorella sp. into 5-hydroxymethylfurfural and levulinic acid by metal sulfate catalyst, Biomass and Bioenergy. 148 (2021) 106053. https://doi.org/10.1016/j.biombioe.2021.106053.

[49] G.T. Jeong, Valorization of microalgae into 5-hydroxymethylfurfural by two-step conversion with ferric sulfate, J. Environ. Manage. 293 (2021) 112919. https://doi.org/10.1016/j.jenvman.2021.112919.

[50] D. Jung, P. Körner, A. Kruse, Kinetic study on the impact of acidity and acid concentration on the formation of 5-hydroxymethylfurfural (HMF), humins, and levulinic acid in the hydrothermal conversion of fructose, Biomass Convers. Biorefinery. 11 (2021) 1155–1170. https://doi.org/10.1007/s13399-019-00507-0.

[51] W. Sailer-Kronlachner, C. Rosenfeld, S. Böhmdorfer, M. Bacher, J. Konnerth, T. Rosenau, A. Potthast, A. Geyer, H.W.G. van Herwijnen, Scale-Up of production of 5-hydroxymethylfurfural-rich adhesive precursors and structural features of humin side products, Biomass Convers. Biorefinery. (2022). https://doi.org/10.1007/s13399-022-03200-x.

[52] N.A.S. Ramli, N.A.S. Amin, Kinetic study of glucose conversion to levulinic acid over Fe/HY zeolite catalyst, Chem. Eng. J. 283 (2016) 150–159. https://doi.org/10.1016/j.cej.2015.07.044.

[53] J. Wang, H. Cui, J. Wang, Z. Li, M. Wang, W. Yi, Kinetic insight into glucose conversion to 5-hydroxymethyl furfural and levulinic acid in LiCl·3H2O without additional catalyst, Chem. Eng. J. 415 (2021) 128922. https://doi.org/10.1016/j.cej.2021.128922.

[54] L. Vilcocq, É. Rebmann, Y.W. Cheah, P. Fongarland, Hydrolysis of Cellobiose and Xylan over TiO2-Based Catalysts, ACS Sustain. Chem. Eng. 6 (2018) 5555–5565. https://doi.org/10.1021/acssuschemeng.8b00486.

[55] R. Rengel, I. Giraldez, M.J. Díaz, T. García, J. Vigara, R. León, Simultaneous production of carotenoids and chemical building blocks precursors from chlorophyta microalgae, Bioresour. Technol. 351 (2022) 127035. https://doi.org/10.1016/j.biortech.2022.127035.

[56] J.L. Vieira, M. Almeida-Trapp, A. Mithöfer, W. Plass, J.M.R. Gallo, Rationalizing the conversion of glucose and xylose catalyzed by a combination of Lewis and Brønsted acids, Catal. Today, 344 (2020) 92-101.

[57] Y. Zhao, S. Wang, H. Lin, J. Chen, H. Xu, Influence of a Lewis acid and a Brønsted acid on the conversion of microcrystalline cellulose into 5-hydroxymethylfurfural in a single-phase

reaction system of water and 1,2-dimethoxyethane, RSC Adv. 8 (2018) 7235–7242. https://doi.org/10.1039/c7ra13387a.

[58] J. Wang, H. Cui, Y. Wang, R. Zhao, Y. Xie, M. Wang, W. Yi, Efficient catalytic conversion of cellulose to levulinic acid in the biphasic system of molten salt hydrate and methyl isobutyl ketone, Green Chem. 22 (2020) 4240–4251. https://doi.org/10.1039/d0gc00897d.

[59] S. Souzanchi, L. Nazari, K.T.V. Rao, Z. Yuan, Z. Tan, C. (Charles) Xu, 5-HMF production from industrial grade sugar syrups derived from corn and wood using niobium phosphate catalyst in a biphasic continuous-flow tubular reactor, Catal. Today. (2021). https://doi.org/10.1016/j.cattod.2021.07.032.

[60] J. Slak, B. Pomeroy, A. Kostyniuk, M. Grilc, B. Likozar, A review of bio-refining process intensification in catalytic conversion reactions, separations and purifications of hydroxymethylfurfural (HMF) and furfural, Chem. Eng. J. 429 (2022). https://doi.org/10.1016/j.cej.2021.132325.

[61] E. V. Dalessandro, J.R. Pliego, Fast screening of solvents for simultaneous extraction of furfural, 5-hydroxymethylfurfural and levulinic acid from aqueous solution using SMD solvation free energies, J. Braz. Chem. Soc. 29 (2018) 430–434. https://doi.org/10.21577/0103-5053.20170140.

[62] B. Saha, M.M. Abu-Omar, Advances in 5-hydroxymethylfurfural production from biomass in biphasic solvents, Green Chem. 16 (2014) 24–38. https://doi.org/10.1039/c3gc41324a.

[63] E.I. Gürbüz, S.G. Wettstein, J.A. Dumesic, Conversion of hemicellulose to furfural and levulinic acid using biphasic reactors with alkylphenol solvents, ChemSusChem. 5 (2012) 383–387. https://doi.org/10.1002/cssc.201100608.

[64] Z. Cao, Z. Fan, Y. Chen, M. Li, T. Shen, C. Zhu, H. Ying, Efficient preparation of 5-hydroxymethylfurfural from cellulose in a biphasic system over hafnyl phosphates, Appl. Catal. B Environ. 244 (2019) 170–177. https://doi.org/10.1016/j.apcatb.2018.11.019.

[65] N. Shi, Y. Zhu, B. Qin, T. Zhu, H. Huang, Y. Liu, Conversion of Cellulose into 5-Hydroxymethylfurfural in a Biphasic System Catalyzed by Aluminum Sulfate and Byproduct Characterization, ACS Sustain. Chem. Eng. 10 (2022) 10444–10456. https://doi.org/10.1021/acssuschemeng.1c08239.

[66] F. Delbecq, Y.T. Wang, C. Len, Various carbohydrate precursors dehydration to 5-HMF in an acidic biphasic system under microwave heating using betaine as a co-catalyst, Mol. Catal. 434 (2017) 80–85. https://doi.org/10.1016/j.mcat.2017.02.037.

[67] J. Teng, H. Ma, F. Wang, L. Wang, X. Li, Catalytic Fractionation of Raw Biomass to Biochemicals and Organosolv Lignin in a Methyl Isobutyl Ketone/H2O Biphasic System, ACS Sustain. Chem. Eng. 4 (2016) 2020–2026. https://doi.org/10.1021/acssuschemeng.5b01338.

[68] N. Sweygers, J. Harrer, R. Dewil, L. Appels, A microwave-assisted process for the in-situ production of 5-hydroxymethylfurfural and furfural from lignocellulosic polysaccharides in a biphasic reaction system, J. Clean. Prod. 187 (2018) 1014–1024. https://doi.org/10.1016/j.jclepro.2018.03.204.

[69] M. Moreno-Recio, I. Jiménez-Morales, P.L. Arias, J. Santamaría-González, P. Maireles-Torres, The Key Role of Textural Properties of Aluminosilicates in the Acid-Catalysed Dehydration of Glucose into 5-Hydroxymethylfurfural, ChemistrySelect. 2 (2017) 2444–2451. https://doi.org/10.1002/slct.201700097.

[70] M. Moreno-Recio, J. Santamaría-González, P. Maireles-Torres, Brönsted and Lewis acid ZSM-5 zeolites for the catalytic dehydration of glucose into 5-hydroxymethylfurfural, Chem. Eng. J. 303 (2016) 22–30. https://doi.org/10.1016/j.cej.2016.05.120.

[71] N. Candu, M. El Fergani, M. Verziu, B. Cojocaru, B. Jurca, N. Apostol, C. Teodorescu, V.I. Parvulescu, S.M. Coman, Efficient glucose dehydration to HMF onto Nb-BEA catalysts, Catal. Today. 325 (2019) 109–116. https://doi.org/10.1016/j.cattod.2018.08.004.